Hindawi
Geofluids
Volume 2019, Article ID 5898901, 13 pages
https://doi.org/10.1155/2019/5898901

Research Article

Sulfate Sources of Thermal Sulfate Reduction (TSR) in the Permian Changxing and Triassic Feixianguan Formations, Northeastern Sichuan Basin, China

Pingping Li,[1,2] **Huayao Zou**,[1,2] **Fang Hao**,[3] **and Xinya Yu**[4]

[1]*State Key Laboratory of Petroleum Resources and Prospecting, China University of Petroleum, Beijing 102249, China*
[2]*College of Geosciences, China University of Petroleum, Beijing 102249, China*
[3]*China University of Petroleum, East China, Qingdao, Shandong 266580, China*
[4]*China University of Geosciences, Wuhan, Hubei 430074, China*

Correspondence should be addressed to Pingping Li; lpp@cup.edu.cn

Received 17 October 2018; Revised 6 January 2019; Accepted 16 January 2019; Published 7 May 2019

Academic Editor: Jean-Luc Michelot

Thermal sulfate reduction (TSR) occurred throughout the Permian Changxing (P_2c) and Triassic Feixianguan (T_1f) dolostone reservoirs in the western and eastern parts of the Kaijiang-Liangping (K-L) trough in the northeastern part of the Sichuan Basin. To determine the sulfate sources of this TSR, fourteen solid bitumen samples and eight anhydrite samples were collected from the northeastern part of the Sichuan Basin. These samples were analyzed to determine their sulfur isotopes. In addition, untreated, HNO_3-treated, and $CrCl_2$-treated solid bitumen samples were analyzed to determine their sulfur isotopes in order to obtain reliable $\delta^{34}S$ data for the TSR solid bitumen. The results show that the HNO_3 method is more effective at removing pyrite from solid bitumen than the method using $CrCl_2$ thrice because the HNO_3-treated solid bitumen has lower sulfur contents and higher $\delta^{34}S$. The $\delta^{34}S$ of the T_1f solid bitumen samples from the Puguang gas field (in the eastern part of the K-L trough, 12.0-24.0‰) is significantly lower than that of the samples from the Yuanba gas field (in the western part of the K-L trough, 24.1-34.2‰). The $\delta^{34}S$ of the T_1f^{1-2} anhydrite is 18.1-26.6‰, which is lower than that of the T_1f^{3-4} anhydrite samples (29.9-39.6‰). The TSR sulfates from the Puguang gas field were most likely from the coeval T_1f^{1-2} evaporating seawater and were enriched during the reflux-seepage dolomitization process. The TSR sulfates from the Yuanba gas field were primarily caused by the evaporation of seawater during the T_1f^4. First, the evaporating seawater would flow vertically into the P_2c reservoirs in the adjacent area, and then, it would flow laterally into the P_2c reservoirs in the Yuanba gas field. Considering the fact that the sulfate sources of TSR and the $\delta^{34}S$ values of the TSR sulfates are different in the Puguang and Yuanba gas fields, the $\delta^{34}S$ of TSR solid bitumen cannot be simply used to show the extent of TSR.

1. Introduction

Thermal sulfate reduction (TSR) is the reaction of sulfate with a hydrocarbon (1) [1, 2]. As toxic and corrosive H_2S can be produced during TSR, the mechanism and products of TSR have been extensively studied [1–4]. The sulfur in the H_2S produced by TSR is derived from dissolved sulfate [1, 3, 5]. Different sulfate sources and whether the sulfates are sufficient or not can affect the H_2S concentration [3, 6] and sulfur isotopic composition of H_2S. Thus, determining the sulfate source is a key problem to predict the H_2S concentration and distribution.

$$\text{Hydrocarbons} + SO_4^{2-} \rightarrow \text{Altered Hydrocarbons} + \text{Solid Bitumen} + CO_2 + H_2S \quad (1)$$

The sulfur in the sulfate is mainly transferred into sulfur-rich solid bitumen, H_2S, and some solid sulfides (such as pyrite) during TSR [7, 8]. The sulfur isotope of sulfur-rich

solid bitumen and H_2S is similar to the sulfur isotope of sulfate [9–11]. Thus, the sulfur isotopes of the sulfur-rich solid bitumen and the H_2S can be used to determine the sulfate source. The sulfur isotopes of the sulfur-rich solid bitumen can be obtained relatively easily compared to those of the toxic H_2S. As a result, we can use the sulfur isotopes of the sulfur-rich solid bitumen to determine the sulfate source.

Pyrite is a byproduct of TSR [1], and it usually resides within the solid bitumen. Thus, we can obtain accurate sulfur isotopes for the solid bitumen only after the pyrite has been removed from the solid bitumen. There are two main methods that can be used to remove pyrite from solid bitumen. One method is to use $CrCl_2$ to reduce the pyrite to H_2S (2) [12]. Cai et al. [13, 14] successfully removed pyrite from kerogen and solid bitumen by this method. The second method is to use dilute HNO_3 to oxidize the pyrite to H_2SO_4 (3) [15, 16]. The $CrCl_2$ method is more complicated than the HNO_3 method, but the HNO_3 method is time consuming. However, there is no research on the use of both methods simultaneously to remove pyrite from solid bitumen, nor has an experiment been conducted to compare the two methods and to determine which method is more effective.

$$FeS_2 + 2CrCl_2 + 4HCl \rightarrow FeCl_2 + 2CrCl_3 + 2H_2S \quad (2)$$

$$FeS_2 + 8HNO_3 \rightarrow Fe(NO_3)_3 + 2H_2O + 2H_2SO_4 + 5NO \quad (3)$$

The relatively high concentration of H_2S (5-20%) in the Permian Changxing (P_2c) and Triassic Feixianguan (T_1f) Formations in the northeastern part of the Sichuan Basin has been concluded to be from TSR [4, 6, 17–19], whereas sulfur-rich solid bitumen has been found in other gas reservoirs [6, 14, 20, 21]. The H_2S concentrations of the gas reservoirs in the eastern part of the Kaijiang-Liangping (K-L) trough (see detailed information in the background section) are higher than those of the gas reservoirs in the western part of the K-L trough [6]. Sulfate from the evaporative platform in T_1f has been suggested as the sulfate source of the TSR [4, 18]. However, whether the sulfate was derived from the early (the first and second members of the T_1f) or late T_1f (the third and fourth members of the T_1f) is unknown. In addition, there is no such evaporative platform in the P_2c in the western part of the K-L trough, so the sulfate source of the TSR in this area is also unknown.

The purpose of this paper is to determine which method is more effective at removing pyrite from solid bitumen by comparing the $CrCl_2$ and HNO_3 methods, to obtain reliable sulfur isotopic data for the solid bitumen, and to analyze the sulfate sources of TSR in the eastern and western parts of the K-L trough in the northeastern part of the Sichuan Basin based on the systematic correlation of the sulfur isotopes of the solid bitumen and anhydrite.

2. Geologic Setting

The Sichuan Basin is a rhombic basin in southwestern China (Figure 1). The general evolutionary history of the Sichuan Basin can be divided into two main stages [22]. Before the Late Indosinian movement, the Sichuan Basin was primarily characterized by subsidence and uplift, and thick marine carbonates and shales were deposited at this stage. Since the Late Indosinian movement, large-scale lateral compression has been occurring, which has resulted in two obvious episodes of uplift, i.e., the Yanshan and Himalayan movements [22]. In addition, terrestrial fluvial-lacustrine deposits were formed.

The Permian strata primarily consist of marine carbonates and shales, and from bottom to top, it can be divided into the Liangshan (P_1l), Qixia (P_1q), Maokou (P_1m), Longtan (P_2l)/Wujiaping (P_2w), and Changxing (P_2c) Formations [22]. The Early Triassic can be divided into the Fexianguan (T_1f) and Jialingjiang (T_1j) Formations, and the T_1f can be furtherly divided into four members (T_1f^1, T_1f^2, T_1f^3, and T_1f^4) from bottom to top. During the P_2c, the northwest-southeast trending K-L trough developed in the northeastern part of the Sichuan Basin (Figure 2). An open platform and a relatively isolated open platform developed in the western and eastern parts of the K-L trough, respectively [23]. During the early T_1f, a restricted evaporative platform (characterized by anhydrite layers) developed in the eastern part of the K-L trough, whereas the western part of the K-L trough was still an open platform and contained no anhydrite layers. Until the end of the T_1f, the evaporative platform remained restricted and widespread anhydrite layers continued to develop in the northeastern part of the Sichuan Basin (Figure 3). The T_1j and Middle Triassic Leikoupo (T_2l) Formations developed on restricted evaporative platforms and consist of limestone and widespread anhydrite [22].

Many gas fields, such as the Puguang, Dukouhe, Tieshanpo, Yuanba, and Longgang, are located in the P_2c and T_1f reefs and shoals in the eastern and western parts of the K-L trough [24, 25]. The natural gas in these gas fields was primarily produced by oil-cracking and was primarily derived from the Upper Permian P_2l/P_2w source rocks [4, 18, 21].

3. Sampling and Analytical Methods

Fourteen solid bitumen-bearing core samples (5 samples from the T_1f in the Puguang gas field and 9 samples from the P_2c in the Yuanba gas field) were collected from the northeast part of the Sichuan Basin, and eight anhydrite samples (7 samples from the T_1f and 1 sample from the T_1j) were collected for this study. The solid bitumen was primarily present as fill in the pores, while the anhydrite primarily occurred as nodules and layers (Figure 4).

The anhydrite nodules and layers were crushed and powdered to less than 100 mesh using an agate mortar and pestle. The solid bitumen-bearing core samples were crushed in a rock crusher to less than 100 mesh, and then, this powder was treated with dichloromethane (DCM) to remove any soluble organic matter and elemental sulfur. The liquid and residue were filtered and flushed with DCM. The residue was dried and treated with hot 6 N HCl to remove carbonate minerals. This solution was heated for 2 hours at 70°C while using a magnetic stirrer. Next, the solid bitumen residue was filtered and rinsed with deionized water, and then, it

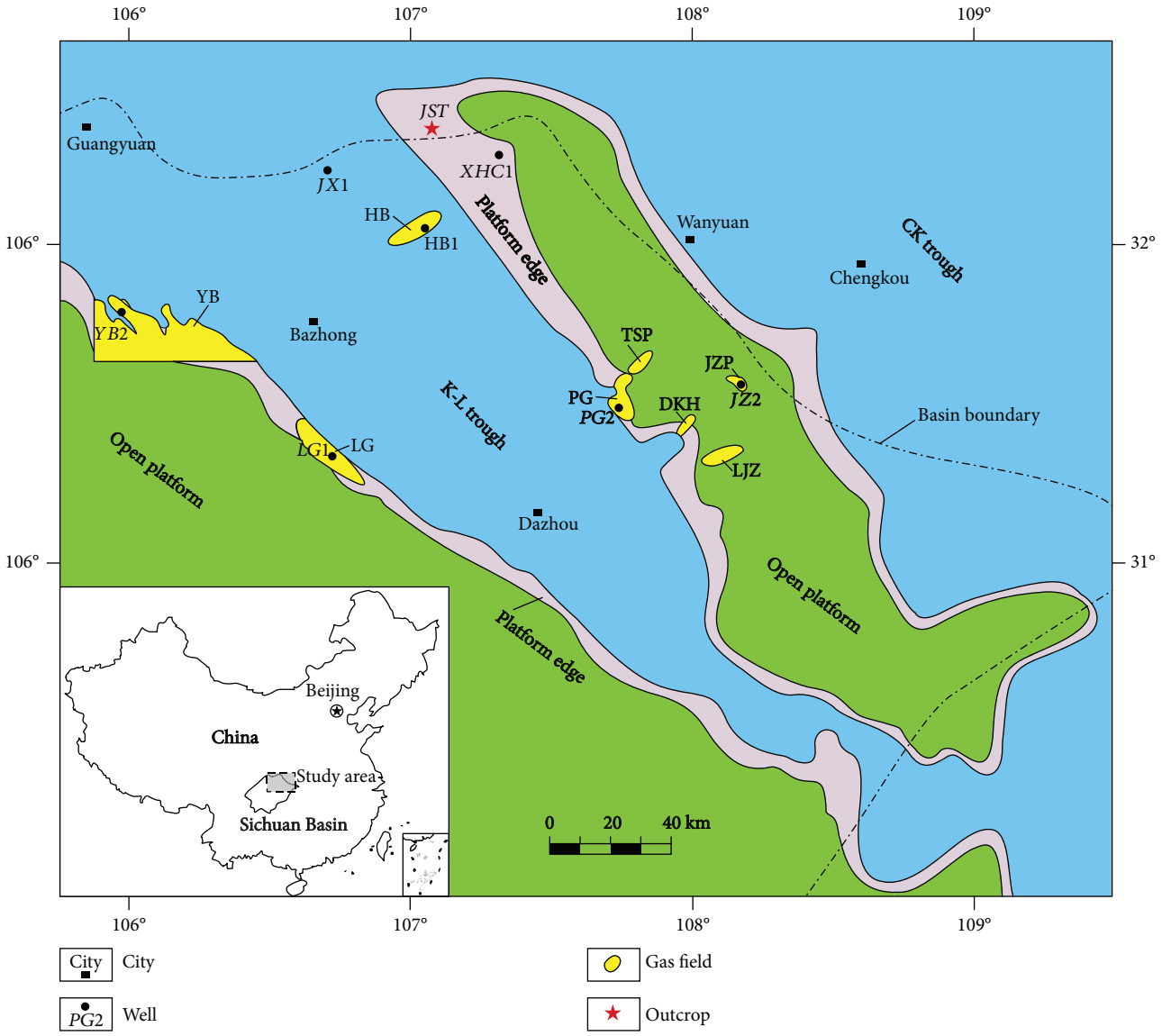

FIGURE 1: Main gas fields and sedimentary facies of the upper part of the Changxing Formation (P_2c) in the northeastern part of the Sichuan Basin (modified from [23, 24]). YB = Yuanba; LG = Longgang; HB = Heba; PG = Puguang; TSP = Tieshanpo; LJZ = Luojiazhai; DKH = Dukouhe; JZP = Jinzhuping; JST = Jiaoshutang; K-L = Kaijiang-Liangping; CK = Chengkou.

was dried at 70°C. The solid bitumen residue was mainly between 100 and 300 mg, so the pyrite content cannot be evaluated precisely using XRD (X-ray diffraction). However, pyrite grains can be easily found using the SEM (Scanning Electron Microscopy) and EDS (Energy Dispersive Spectrometer) analysis (Figure 5). As a result, it is necessary to remove pyrite to get accurate sulfur isotope of the solid bitumen. So the solid bitumen residue was treated with HNO_3 and $CrCl_2$ to remove the pyrite, respectively.

The HNO_3 method requires the solid bitumen residue to react with 1 N HNO_3 in a glass centrifuge tube at room temperature for two weeks. The centrifuge tubes were sonicated for 30 minutes every day. After reacting with 1 N HNO_3 for two weeks, deionized water was added to the tubes, they were centrifuged again, and the liquid was poured off. This procedure was repeated twice more. Finally, the solid bitumen was dried at 70°C for 12 hours.

The $CrCl_2$ method used was similar to the method reported by Cai et al. [13, 14]. First, 12 N HCl and deionized water were added to solid $CrCl_3 \cdot 6H_2O$ to prepare a green $CrCl_3$ solution. Then, the green $CrCl_3$ solution was allowed to slowly flow past a flask column filled with granular zinc to convert it to a dark blue $CrCl_2$ solution, which was stored in a ground glass stoppered bottle to prevent oxidation. Next, 6 N HCl and the $CrCl_2$ solution were added to the solid bitumen residue in a glass tube, and then, the tube was covered with a plastic cap with a syringe needle, which allowed the generated H_2S to flow out. The tube was heated at 80°C for 3 hours, then deionized water was added, the tube was centrifuged twice, the liquid was poured off, and the solid bitumen

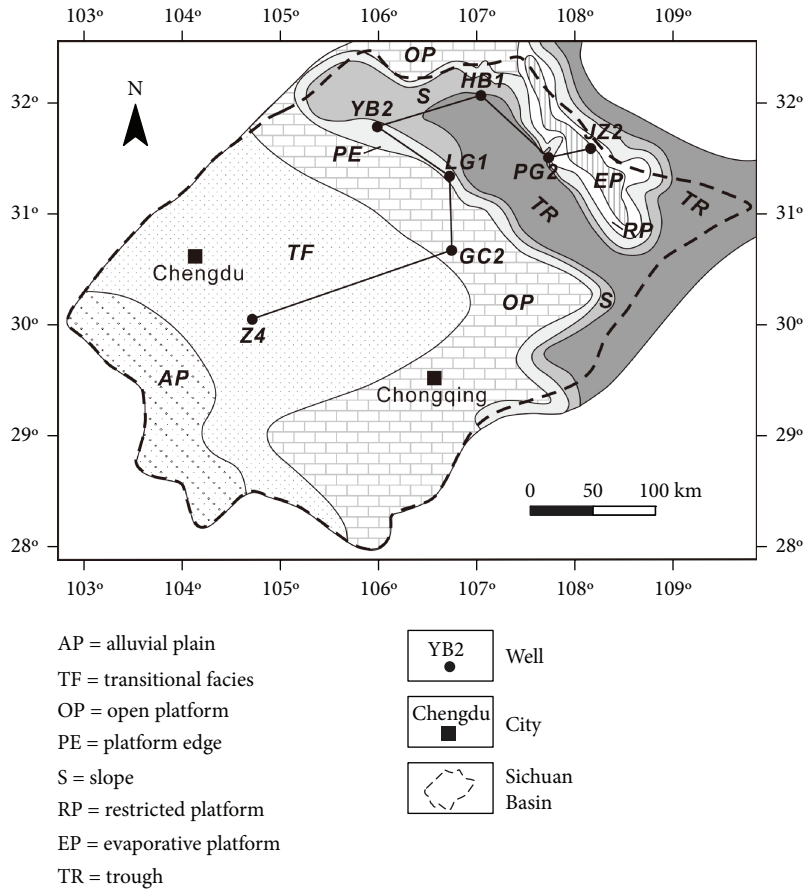

FIGURE 2: Key wells and sedimentary facies in the upper part of the second member of the Feixianguan Formation (T_1f^2) in the Sichuan Basin (modified from [24]).

residue was reground. Finally, this procedure was repeated twice, and the solid bitumen was dried.

The sulfur isotopes of the anhydrite powder, the untreated solid bitumen residue, and the HNO_3-treated and $CrCl_2$-treated solid bitumen were analyzed at the California Institute of Technology. Samples were combusted in a Costech elemental combustion system at 1000°C, and then, the isotopic ratios were determined using a Delta Plus XL mass spectrometer calibrated using International Atomic Energy Agency (IAEA) standards. The results are reported as $\delta^{34}S$ relative to the Vienna Canyon Diablo Troilite (VCDT) standard. Average precision of analyses based on replicate analyses of standards was ±0.2‰.

4. Results

4.1. Sulfur Content and Isotope Ratios of the Solid Bitumen Samples. The sulfur contents and sulfur isotopes ($\delta^{34}S$) of the untreated solid bitumen, the HNO_3-treated solid bitumen, and the $CrCl_2$-treated solid bitumen are listed in Table 1. As the weight of the untreated solid bitumen is small, two samples (SB10 and SB12) were not treated with $CrCl_2$.

The sulfur contents of the untreated solid bitumen, the HNO_3-treated solid bitumen, and the $CrCl_2$-treated solid bitumen were different (Figure 6). Except for one sample (SB16), the sulfur contents of the HNO_3-treated and $CrCl_2$-treated solid bitumen samples were lower than those of the untreated solid bitumen samples. In addition, the sulfur contents of the HNO_3-treated and $CrCl_2$-treated solid bitumen samples were similar, but the sulfur contents of three of the HNO_3-treated solid bitumen samples (SB2, SB5, and SB13) were lower than those of the $CrCl_2$-treated solid bitumen samples (Figure 6).

Similarly, the $\delta^{34}S$ values of the untreated solid bitumen samples, the HNO_3-treated solid bitumen samples, and the $CrCl_2$-treated solid bitumen samples were different (Figure 7). Except for two samples (SB4 and SB11), the $\delta^{34}S$ values of the untreated solid bitumen samples were lower than those of the HNO_3- and $CrCl_2$-treated solid bitumen samples. In addition, the $\delta^{34}S$ values of the HNO_3- and $CrCl_2$-treated solid bitumen samples were similar. However, in the case of samples SB2, SB5, SB13, and SB17, the $\delta^{34}S$ values of the HNO_3-treated solid bitumen samples were higher than those of the $CrCl_2$-treated solid bitumen samples (Figure 7), while the sulfur contents of the HNO_3-treated solid bitumen samples were lower than those of the $CrCl_2$-treated solid bitumen samples (Figure 6). The $\delta^{34}S$ difference between these four HNO_3-treated solid bitumen samples and corresponding untreated solid bitumen was 3.2‰, 4.4‰, 9.7‰, and 1.8‰, respectively, and the $\delta^{34}S$ difference

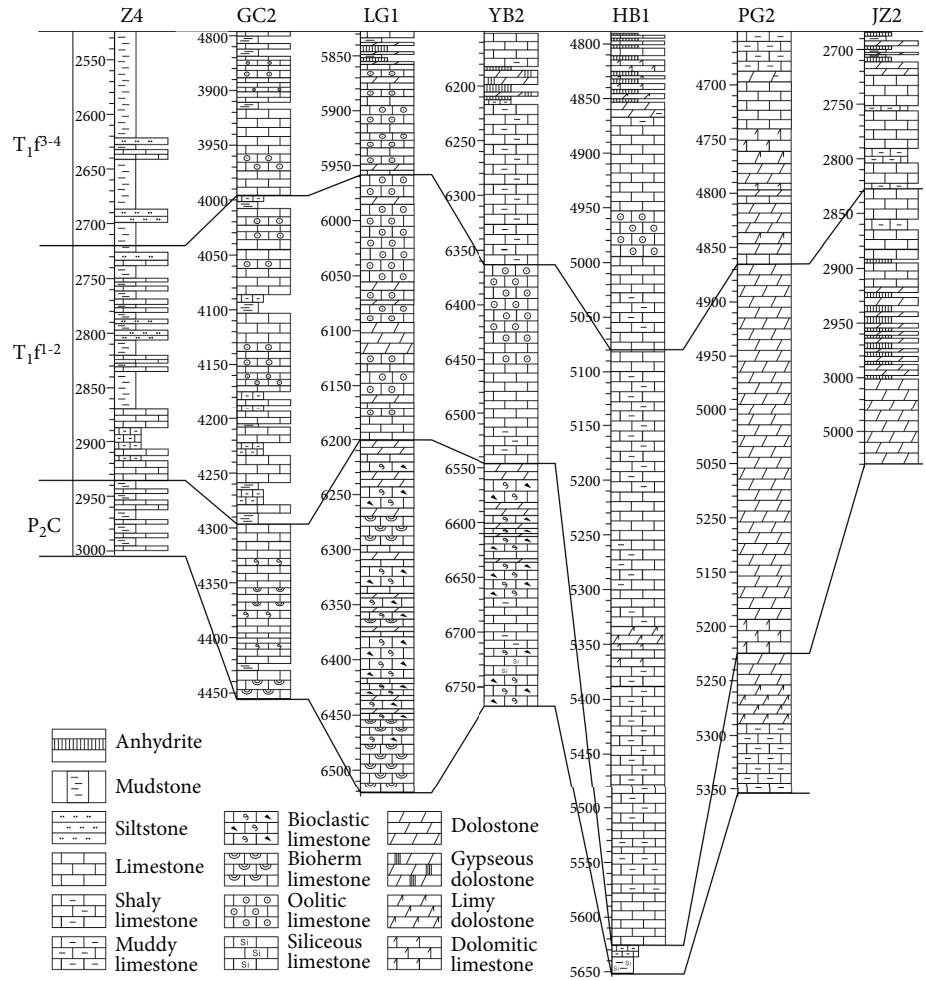

FIGURE 3: The lithologic variations in the Changxing (P_2c) and Feixianguan (T_1f) Formations in the Sichuan Basin from southwest to northeast. The data for wells Z4, GC2, LG1, and JZ2 are from Du et al. [24]. The figures to the left of each lithologic column are the burial depths (in m). T_1f^{1-2} = the first and second members of T_1f; T_1f^{3-4} = the third and fourth members of T_1f. The well locations are shown in Figure 2.

between these four $CrCl_2$-treated solid bitumen samples and corresponding untreated solid bitumen were 1.2‰, 3.6‰, 7.3‰, and 1.6‰, respectively.

Overall, there is no obvious difference in the sulfur contents of the solid bitumen samples from the Puguang and Yuan gas fields, and the sulfur contents ranged from 4.0% to 15.0% (Figure 6), which are roughly similar to the sulfur content ranges reported for solid bitumen from the Puguang gas field (11.75-11.99%; [4]) and from the Yuanba gas field (6.64-17.99%; [6]). However, the $\delta^{34}S$ of solid bitumen from the Puguang gas field (generally lower than 20.0‰) is significantly lower than that of solid bitumen from the Yuanba gas field (generally higher than 24.0‰).

4.2. Sulfur Isotope Ratios of the Anhydrite Samples. The $\delta^{34}S$ of the eight anhydrite samples analyzed and the $\delta^{34}S$ reported for other anhydrites are listed in Table 2.

For the eight anhydrites analyzed in this study, the $\delta^{34}S$ of the T_1f^1 anhydrite (26.2–26.6‰) was lower than that of the T_1f^3–T_1f^4 anhydrites (29.9-34.4‰) and the T_1j anhydrite (31.7‰). The $\delta^{34}S$ of the T_1f^1 anhydrite is similar to the $\delta^{34}S$ range reported for the T_1f^1–T_1f^3 anhydrites (18.12-30.7‰; [19, 26]), and the $\delta^{34}S$ of the T_1f^4 anhydrite is close to that reported for the T_1f^4 anhydrite (35.88-39.64‰, [27]) and the T_1j anhydrite (24.7-32.5‰, [28]; 29.72‰, [27]). This suggests that the $\delta^{34}S$ values of the anhydrite samples are reliable. The $\delta^{34}S$ of the T_1f^1–T_1f^3 anhydrites (18.12-30.7‰) reported by Wang et al. [26] and Zhu et al. [19] is mainly for the T_1f^1–T_1f^2 because the anhydrite was mainly located within the T_1f^1–T_1f^2 in the Dukouhe, Tieshanpo, and Jinzhuping gas fields (Figure 3).

Overall, the $\delta^{34}S$ of the T_1f^1–T_1f^2 anhydrites (18.12-26.6‰) was lower than that of the T_1f^3–T_1f^4 anhydrites (29.9-39.6‰), which is consistent with the conclusion that the $\delta^{34}S$ of seawater sulfate increased during the Early Triassic [29].

5. Discussion

5.1. Which Method Is More Effective at Removing Pyrite from Solid Bitumen? Pyrite can be a byproduct of TSR [1, 8]. Pyrite grains were observed in the T_1f reservoir cores and have been

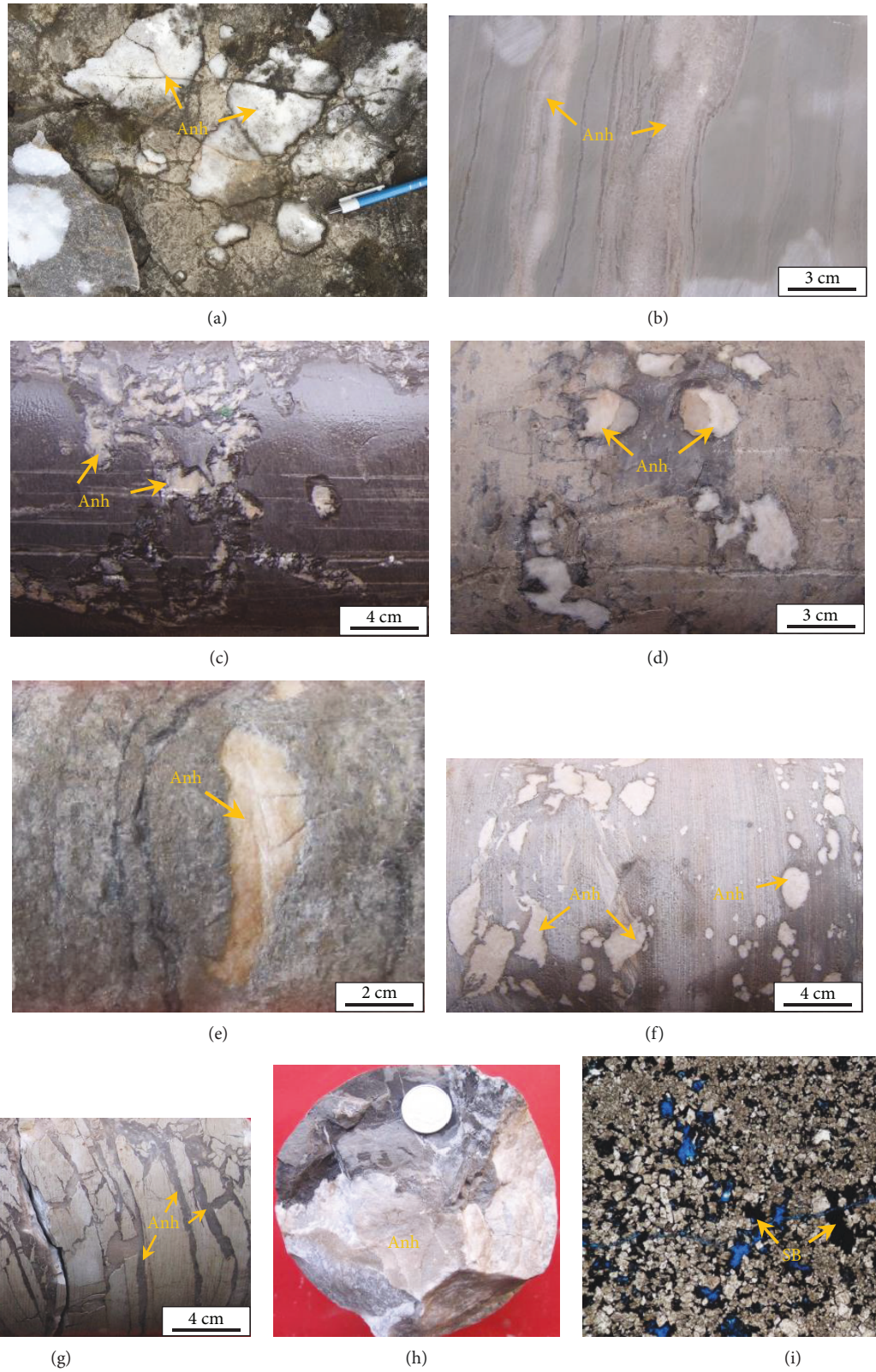

Figure 4: Photographs showing anhydrite (Anh) in an outcrop sample (a) and in cores (b–h), and black solid bitumen in thin section (i). (a) Outcrop JST, T_1f^4, anhydrite nodules in dolostone. (b) Well HB1, 4847.6 m, T_1f^4, anhydrite layers in mudstone. (c) Well HB1, 4501 m, T_1j^2 (second member of the Jialingjiang Formation), anhydrite nodules in dolostone. (d) Well MB6, 4015.9 m, T_1f^1, anhydrite nodules in limestone. (e) Well XHC1, 5468.2 m, T_1f^1, anhydrite nodules in dolostone. (f) Well DW2, 4750.7 m, T_1f^3, anhydrite nodules in dolostone. (g) Well MB1, 4302.3 m, T_1f^4, anhydrite layers in mudstone. (h) Well MB3, 3873 m, T_1f^4, large anhydrite nodules in dolostone. (i) Well YB271, 6327.4 m, P_2c, black solid bitumen in the pores.

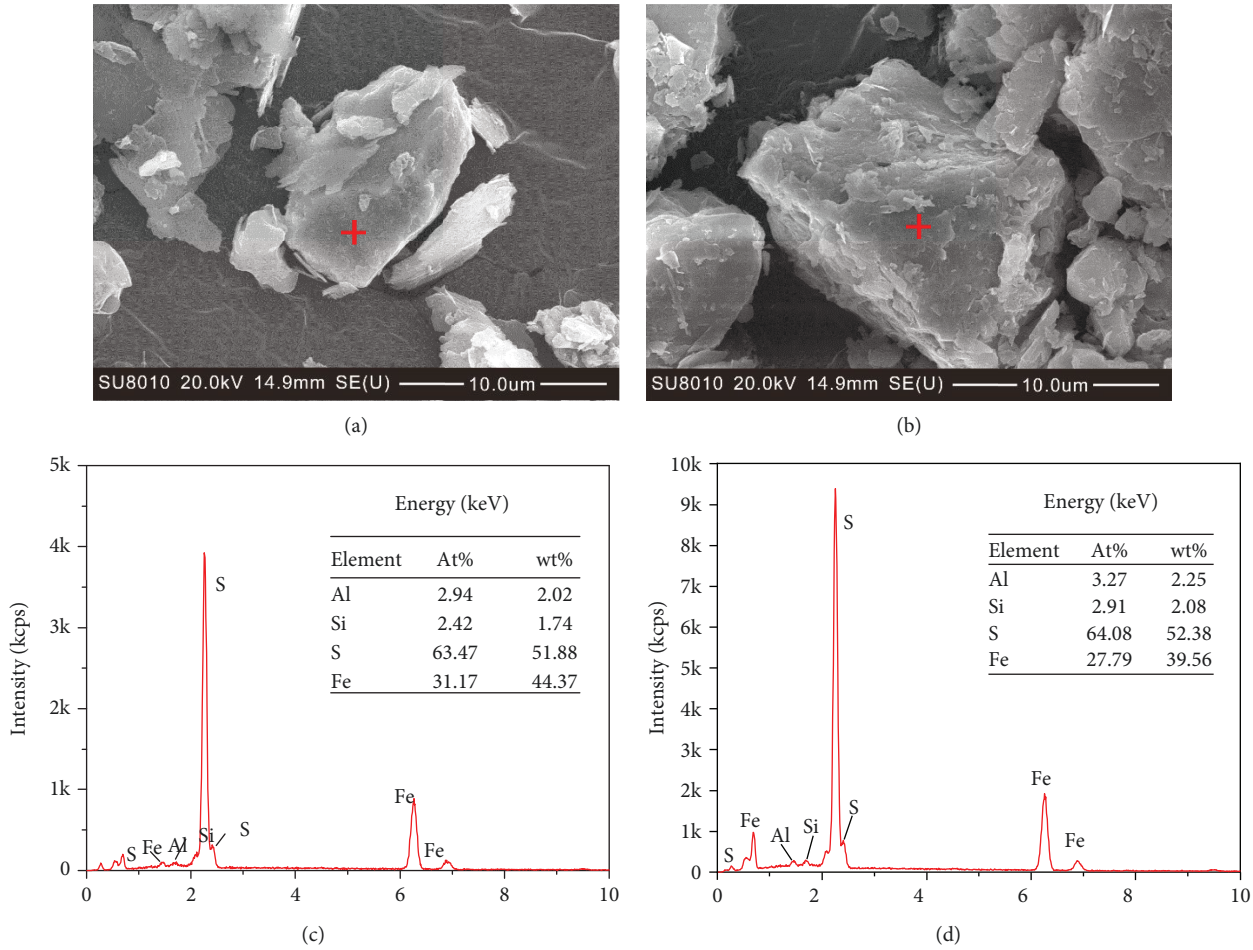

Figure 5: SEM (Scanning Electron Microscopy) and EDS (Energy Dispersive Spectrometer) photographs showing pyrites in the untreated SB2 (a, c) and SB13 (b, d) solid bitumen samples.

suggested to be formed by TSR because their $\delta^{34}S$ is 18.7-20.16‰ [19], which differs from that of the pyrite from the source rock layers. Except for one sample (SB16), the sulfur contents of the HNO_3-treated and $CrCl_2$-treated solid bitumen samples are lower than those of the untreated solid bitumen samples (Figure 6), which support the conclusion that some of the sulfur was removed by the HNO_3 and $CrCl_2$ methods. The untreated solid bitumen samples were extracted by DCM so that the organic matter and elemental sulfur were removed from the solid bitumen. As a result, the decrease in the sulfur contents of the HNO_3-treated and $CrCl_2$-treated solid bitumen samples was most likely caused by the removal of some of the pyrite. In addition, the special smell of released H_2S was smelled when the solid bitumen was treated with $CrCl_2$, and small pyrite grains were observed in the untreated solid bitumen powder with SEM (Figure 5). XRD had been used to determine the pyrite content in kerogen and solid bitumen [13, 14], and an improved method to determine the pyrite content by measuring the dissolved iron at $pH < 2$ using an atomic absorption spectrometer was developed by Cai et al. [30]. However, XRD and the dissolved iron analysis were not performed in this study because the obtained untreated solid bitumen samples weighed less than 100–300 mg each, so the pyrite content could not be determined. However, it is reasonable that the decrease in the sulfur contents of the HNO_3- and $CrCl_2$-treated solid bitumen samples was caused by removing some of the pyrite.

Approximately 88.9-99.7% of pyrite was removed when the kerogen was treated twice with $CrCl_2$ [12]. Cai et al. [13, 14, 30] used a similar method and successfully removed the pyrite from kerogen and solid bitumen samples, and sulfur isotopes were analyzed only when pyrite sulfur/total sulfur values were less than 0.08 [30]. However, no studies have been conducted to compare the HNO_3 and $CrCl_2$ methods. In this study, the sulfur contents and sulfur isotopes of most of the solid bitumen samples treated using the HNO_3 and $CrCl_2$ methods were quite similar (Figures 6 and 7), which demonstrate that pyrite was removed by both methods. However, some of the HNO_3-treated solid bitumen samples (SB2, SB5, SB13, and SB17) had significantly lower sulfur contents and significantly higher $\delta^{34}S$ than the $CrCl_2$-treated solid bitumen samples (Figure 6), which suggests that the HNO_3 method is more effective at removing pyrite from solid bitumen than the method using $CrCl_2$ thrice. In particular, the $\delta^{34}S$ of the $CrCl_2$-treated sample SB13 (16.8‰) is still less than 20.0‰, but it is 2.4‰ higher than that of untreated sample SB13. The $\delta^{34}S$ of HNO_3-treated sample SB13 is 24.1‰, which is similar to the $\delta^{34}S$

Table 1: Sulfur content and isotope composition of solid bitumen from the Yuanba and Puguang gas fields in the Sichuan Basin.

Gas field	Well	Sample no.	Strata	Depth (m)	Untreated SB		$CrCl_2$-treated SB		HNO_3-treated SB	
					S%	δ^{34}S‰	S%	δ^{34}S‰	S%	δ^{34}S‰
Puguang	MB4	SB1	T_1f^2	3814.5	12.41	17.6	10.47	17.5	11.04	17.9
Puguang	MB4	SB2	T_1f^2	3836.3	6.18	15.4	5.76	16.6	4.63	17.8
Puguang	PG12	SB3	T_1f^2	6007.5	8.17	16.9	7.52	18.1	7.58	17.9
Puguang	PG2	SB4	T_1f^1	5059.0	11.53	20.1	10.57	19.0	10.54	18.5
Puguang	DW102	SB5	T_1f^1	4819.7	5.68	13.3	5.04	14.1	3.51	17.7
Yuanba	YB29	SB7	P_2c	6642.4	12.4	27.7	11.6	27.9	12.1	28.5
Yuanba	YB205	SB8	P_2c	6461.4	9.37	34.2	7.92	34.3	7.89	34.2
Yuanba	YB27	SB10	P_2c	6295.3	11.53	25.9	/	/	11.08	26.5
Yuanba	YB27	SB11	P_2c	6301.1	10.17	31.1	8.87	29.8	8.89	29.4
Yuanba	YB273	SB12	P_2c	6826.2	10.34	25.1	/	/	10.29	25.6
Yuanba	YB271	SB13	P_2c	6320.5	9.87	14.4	7.55	16.8	4.52	24.1
Yuanba	YB28	SB15	P_2c	6807.3	11.75	30.5	11.6	29.8	11.1	30.3
Yuanba	YB224	SB16	P_2c	6627.9	10.34	25.2	13.4	25.4	12.77	25.9
Yuanba	YB224	SB17	P_2c	6641.2	14.57	24.7	14.28	24.9	13.66	26.5

Note: P_2c = Changxing Formation (Fm); T_1f^1 = the first member of Feixianguan Fm; T_1f^2 = the second member of Feixianguan Fm.

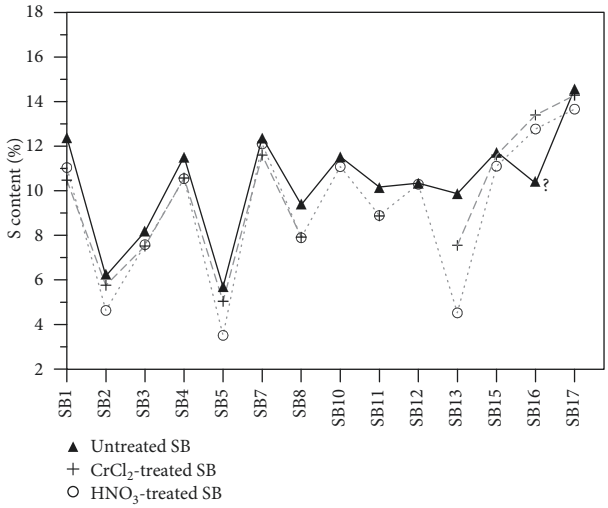

Figure 6: Variation in the sulfur contents of the untreated, $CrCl_2$-treated, and HNO_3-treated solid bitumen (SB) samples.

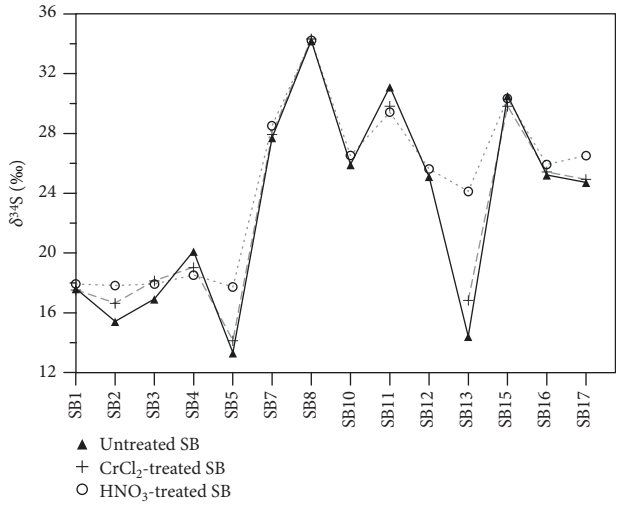

Figure 7: Variations in the sulfur isotopes of the untreated, $CrCl_2$-treated, and HNO_3-treated solid bitumen (SB) samples.

of the other HNO_3-treated solid bitumen samples from the Yuanba gas field (greater than 24.0‰) (Figure 7). Therefore, the δ^{34}S of HNO_3-treated sample SB13 should be closer to that of solid bitumen without pyrite. In addition, the difference in sulfur content (ΔS) and the difference in the sulfur isotopes ($\Delta\delta^{34}$S) of the HNO_3- and $CrCl_2$-treated solid bitumen samples are negatively correlated ($R^2 = 0.83$; Figure 8), indicating that the δ^{34}S of the HNO_3-treated solid bitumen samples increases more with decreasing sulfur content than the δ^{34}S of the $CrCl_2$-treated samples does. This also supports that the HNO_3 method is more effective at removing pyrite from solid bitumen than the method using $CrCl_2$ thrice.

As a result, the δ^{34}S of the solid bitumen discussed in the next section is the δ^{34}S of the HNO_3-treated solid bitumen samples. Though we cannot be absolutely sure that all of the pyrite was completely removed from the solid bitumen by the HNO_3 method, we believe that the δ^{34}S of the HNO_3-treated solid bitumen samples is quite similar to the true δ^{34}S of solid bitumen without pyrite. Thus, the δ^{34}S of solid bitumen samples can be used to investigate the origin of the sulfur.

5.2. Sulfate Sources of TSR. The solid bitumens from the T_1f and P_2c reservoirs in the northeastern part of the Sichuan Basin are insoluble pyrobitumens, which were formed in the advanced stages of thermal maturity [4, 21]. Insoluble solid bitumen can form due to the thermal chemical alteration (TCA) or thermochemical sulfate reduction (TSR) of migrated petroleum [31]. The S/C ratio of TSR bitumen is

Table 2: Sulfur isotope compositions of anhydrite from the northeastern Sichuan Basin.

Area/gas field	Well	Strata	Depth (m)	Sample description	$\delta^{34}S$/‰
XHC	XHC1	T_1f^1	5468.2	Anhydrite layer	26.2
PG	MB6	T_1f^1	4015.9	Anhydrite nodule	26.6
PG	DW2	T_1f^3	4750.7	Anhydrite nodule	29.9
HB	HB1	T_1f^4	4847.6	Anhydrite layer	34.3
PG	MB1	T_1f^4	4302.3	Anhydrite nodule	34.2
PG	MB3	T_1f^4	3873.0	Anhydrite nodule	34.4
JST	JST	T_1f^4	/	Anhydrite nodule	34.0
HB	HB1	T_1j^2	4501.0	Anhydrite layer	31.7
DKH*	Du3	T_1f^{1-3}	/	Anhydrite layer	26.5
DKH*	Du3	T_1f^{1-3}	/	Anhydrite nodule	30.0
DKH*	D4	T_1f^{1-3}	/	Anhydrite nodule	30.7
TSP*	Po1	T_1f^{1-3}	/	Anhydrite nodule	30.1
TSP*	Po1	T_1f^{1-3}	/	Anhydrite nodule	30.6
HB#	HB102	T_1f^3	5176.8	Anhydrite vein	34.3
PG#	MB6	T_1f^1	4015.7	Anhydrite nodule	26.48
HB#	HB1	T_1f^4	4847.3	Anhydrite layer	35.88
PG#	MB2	T_1f^4	4144.0	Anhydrite layer	39.33
JZP†	Z2	T_1f	3416.8	Anhydrite	19.71
LJZ†	Lj2	T_1f^{1-3}	2897.2	Anhydrite	22.59
DKH†	Du3	T_1f^{1-3}	4290.0	Anhydrite	18.12
DKH†	Du5	T_1f^{1-3}	4740.3	Anhydrite	24.34
DKH†	Du5	T_1f^{1-3}	4742.3	Anhydrite	22.8
DKH†	Du5	T_1f^{1-3}	4753.4	Anhydrite	22.83
TSP†	Po1	T_1f^{1-3}	3302.7	Anhydrite	19.46
TSP†	Po3	T_1f^{1-3}	3464.7	Anhydrite	18.92
QLX†	QL52	T_1f^{1-3}	3536.0	Anhydrite	24.64
QLX†	QL52	T_1f^{1-3}	3490.4	Anhydrite	23.57
JZP†	JZ1	T_1f^{1-3}	2825.8	Anhydrite	19.35
JZP†	JZ1	T_1f^{1-3}	2877.2	Anhydrite	22.07
JZP†	JZ1	T_1f^{1-3}	4766.0	Anhydrite	22.13
JZP†	ZJ1	T_1f^{1-3}	3941.9	Anhydrite	23.74
JZP†	Z1	T_1f^{1-3}	3350.5	Anhydrite	18.09
JZP†	Z1	T_1f^{1-3}	5648.9	Anhydrite	25.4
PG††	MB3	T_1f^4	3872.0-3880.2	Anhydrite vein	39.64
PG††	MB3	T_1f^4	3872.0-3880.2	Anhydrite vein	38.56
PG††	CY83	T_1j^4	3552.0-3554.0	Anhydrite layer	29.72

*from Wang et al. [26], #from Zhang [39], †from Zhu et al. [19], ††from Zhu et al. [27].

generally greater than 0.03 [31], while its $\delta^{34}S$ is close to the $\delta^{34}S$ of sulfate [11, 32, 33]. The S/C ratio of TCA bitumen is generally less than 0.03 [31], while its $\delta^{34}S$ is similar to the $\delta^{34}S$ of the source kerogen [20]. The S/C ratios of the T_1f and P_2c solid bitumen from the Puguang and Yuanba gas fields are greater than 0.03 [4, 6]. In addition, the $\delta^{34}S$ of this solid bitumen is 12.0-35.0‰ (Figure 9), which is significantly higher than that of the kerogen from the Permian source rocks from well HB1 (−26.7‰; [30]), but it is close to the $\delta^{34}S$ of the T_1f anhydrite (18.0-35.0‰; Figure 9). The S/C ratios and the $\delta^{34}S$ values of the solid bitumen both support its TSR origin.

The mechanism by which the sulfur in the sulfate is transferred into the solid bitumen is not yet clearly understood. However, when the TSR proceeds gradually, the saturate/aromatic ratio of the TSR-altered oil decreases, while the sulfur and oxygen contents of the solid bitumen increase [32, 34], which suggests that the sulfur was transferred from the sulfate into the hydrocarbon. In addition, the TSR-altered oils are rich in sulfur compounds, such as thiophenes, benzothiophens, and dibenzothiophenes [32, 33]. The isotopic fractionation of sulfur that occurs during the TSR process is minimal, so the $\delta^{34}S$ of the TSR-altered oil and solid bitumen is close to that of the TSR-involved sulfate [9–11, 28, 32, 33].

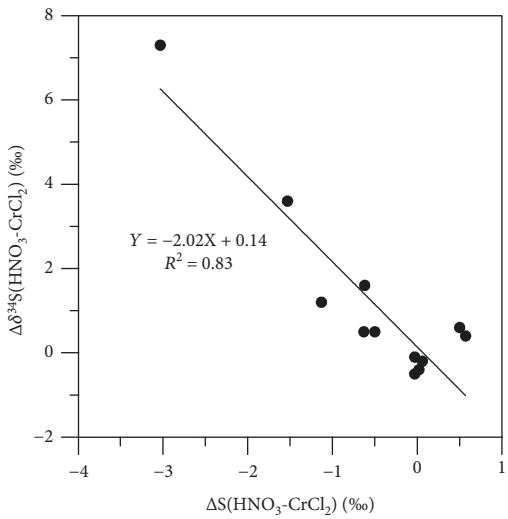

Figure 8: Variation in differences in the sulfur contents (ΔS) and the differences in the sulfur isotopes ($\Delta\delta^{34}S$) of the HNO_3-treated and $CrCl_2$-treated solid bitumen samples.

TSR can occur in both gas zone and gas-water transition zone [17], but the sulfur fractionations were different in these two zones [14]. In the gas-water transition zone, the gas saturation was low so that some dissolved sulfate remains unreacted, and the TSR solid bitumen would be enriched in $\delta^{34}S$ and H_2S would be depleted in $\delta^{34}S$. In the gas zone, the limited dissolved sulfate would be reduced completely, so that the $\delta^{34}S$ of TSR solid bitumen would be close to the $\delta^{34}S$ of sulfate. However, the solid bitumen samples from the Yuanba and Puguang gas fields were both collected from present gas zones, so we considered that the sulfur fractionation during the TSR was insignificant.

As shown in Figure 9, the $\delta^{34}S$ of the solid bitumen from the Puguang gas field in the eastern part of the K-L trough is generally less than 24.0‰ (except for one sample with 31.2‰), whereas the $\delta^{34}S$ of the solid bitumen from the Yuanba gas field in the western part of the K-L trough is generally greater than 24.0‰ (24.1-34.2‰). Thus, assuming minimal isotopic fractionation of sulfur during TSR, it is impossible for the sulfur in the solid bitumen from the Yuanba gas field to have come from the T_1f^1 and T_1f^2 sulfates because the $\delta^{34}S$ of these sulfates is lower than that of the solid bitumen. However, the $\delta^{34}S$ of the solid bitumen is similar to that of the T_1f^3 and T_1f^4 anhydrites. In addition, there is no anhydrite in T_1f^1 and T_1f^2 in the Yuanba gas field, and the anhydrite is only present in T_1f^4 (Figure 3). As a result, the sulfate of the TSR was most likely from T_1f^4 in the Yuanba gas field. The primary source of the sulfate of the TSR in the Puguang gas field was the T_1f^1 and T_1f^2 anhydrite layers, which have slightly higher $\delta^{34}S$ than the solid bitumen, but part of the sulfate was from the T_1f^3 and T_1f^4 anhydrite layers because the $\delta^{34}S$ of some of the solid bitumen is higher than that of the T_1f^1 and T_1f^2 anhydrites (Figure 9). Based on the correlation between the $\delta^{34}S$ values of the solid bitumen and anhydrite samples, it can be concluded that the sulfate source of the TSR is different in the western and eastern parts of the K-L trough.

The H_2S-rich natural gases of the T_1f and P_2c are mainly located in the dolostone reservoirs in the northeastern part of the Sichuan Basin, whereas no H_2S was found in limestone reservoirs [6]. Thus, we suggest that the TSR sulfates (including anhydrites and dissolved sulfates) were enriched during the dolomitization process. Geological observations and numerical simulations have demonstrated that anhydrite can be a byproduct of the dolomitization process [35, 36], which indicates that sulfates can be enriched during the dolomitization process. According to the calculations by Li et al. [6], if all of the SO_4^{2-} in the formation water were converted to H_2S during TSR, the generated H_2S concentration would be 8.8-23.3%, which is similar to the range observed in the Puguang (5.09–19.22%, [4]) and Yuanba (1.20-12.16%, [6]) gas fields. In addition, the anhydrite produced in the dolomitization process can also supply additional sulfates. TSR calcites have been observed to replace anhydrite in the T_1f dolostone reservoir in the northeastern part of the Sichuan Basin [19]. Therefore, the sulfates enriched during the dolomitization process can supply sufficient sulfur to produce the observed H_2S concentration in the northeastern part of the Sichuan Basin.

The sulfates of the TSR in the Puguang gas field in the eastern part of the K-L trough were most probably enriched during the reflux-seepage dolomitization process [37–39]. The coevally evaporating seawater of the T_1f flowed laterally into the porous T_1f oolitic limestone and the P_2c reef limestone, causing broad dolomitization, during which the TSR sulfates (anhydrites and dissolved sulfates) were enriched. The down migration model of dolomitization fluid from T_1f and P_2c had been supported by the evidence that the P_2c dolostones have $^{87}Sr/^{86}Sr$ ratios close to the ratios of T_1f seawater but heavier than P_2c seawater [38]. This is similar to the Permian Khuff Formation, offshore Dubai [40]. Finally, the sulfur from the sulfates was transferred into the solid bitumen and the H_2S. The SO_4^{2-} concentration of the formation water from the Puguang gas field (H_2S concentration of 10-20%) is less than 1.0 g/L, which is far lower than that of the formation water from the Jiannan gas field (H_2S concentration less than 5%), indicating that the dissolved sulfates in the formation water were consumed during the TSR process in the Puguang gas field [6].

As was previously discussed, the sulfates of the TSR in the Yuanba gas field were most likely from the evaporating seawater in T_1f^4. However, the micritic limestone of T_1f^1 and T_1f^2 can act as a barrier to prevent evaporating seawater of T_1f^4 from flowing vertically into the P_2c reservoirs (Figure 3). However, there are porous dolostone reservoirs in T_1f^1 and T_1f^2 in the Longgang gas field (Figure 3), which is also in the western part of the K-L trough and adjacent to the Yuanba gas field, so we suggest that the evaporating seawater may have initially flowed vertically from T_1f^4 into T_1f^1 and T_1f^2, then it flowed into the P_2c reservoir layers in the Longgang gas field, and finally, it flowed laterally into the P_2c reservoirs in the Yuanba gas field, which caused the dolomitization and enrichment of the sulfates of the TSR.

Cai et al. [30] proposed that the $\delta^{34}S$ and S/C ratio of the TSR solid bitumen samples can be used to show the TSR extent based on systematic analysis of TSR and non-TSR

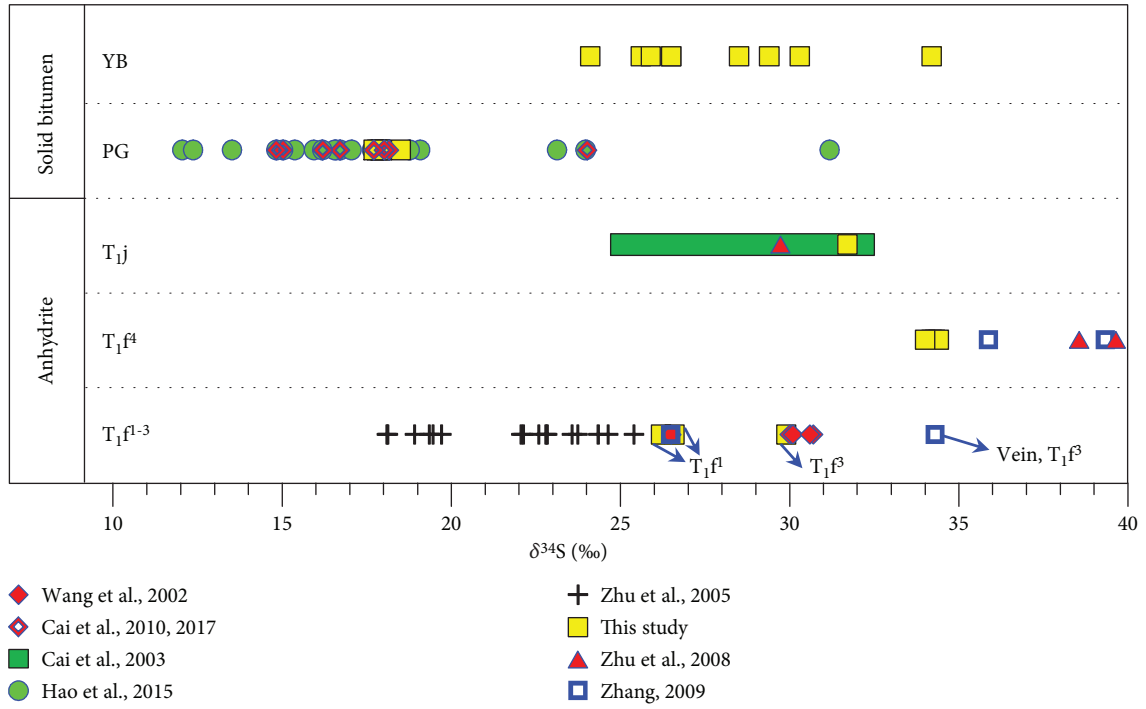

Figure 9: Correlation between the sulfur isotopes of the solid bitumen and anhydrite samples in the northeastern part of the Sichuan Basin.

solid bitumen samples in the northeastern part of the Sichuan Basin. However, the $\delta^{34}S$ values of the P_2c solid bitumen in the western part of the K-L trough, such as those from the Yuanba and Longgang gas fields, are not included in that paper. As was previously discussed, the $\delta^{34}S$ of the solid bitumen from the Yuanba gas field is significantly higher than that from the Puguang gas field. However, the S/C of the solid bitumen from the Yuanba gas field (less than 0.06) is less than the S/C of the solid bitumen from the Puguang gas field (greater than 0.06). Also, the H_2S concentration of the Yuanba gas field (5-10%) is lower than that of the Puguang gas field (10-20%), and the corresponding GSI (gas sourcing index), which was used to reflect the extent of TSR [41], is lower in the Yuanba gas field (less than 0.1) than in the Puguang gas field (0.1-0.2). Thus, we conclude that the extent of TSR was greater in the Puguang gas field than in the Yuanba gas field. As a result, we suggest that the $\delta^{34}S$ of TSR solid bitumen can be used as an indicator of the TSR extent only when the sulfate source of the TSR is similar ($\delta^{34}S$ of sulfate source is similar).

6. Conclusions

The following conclusions can be drawn based on our study:

(1) Both the HNO_3 method and the $CrCl_2$ method successfully remove pyrite from solid bitumen, but the HNO_3 method is more effective than the method using $CrCl_2$ thrice

(2) The $\delta^{34}S$ of the T_1f solid bitumen from the Puguang gas field (12.0-24.0‰) is lower than the $\delta^{34}S$ of the P_2c solid bitumen from the Yuanba gas field (24.1-34.2‰), and the sulfates of the TSR of the Puguang gas field were mainly formed by evaporating seawater in T_1f^{1-2}, whereas the sulfates of the TSR in the Yuanba gas field were mainly formed by evaporating seawater in T_1f^4

(3) When the $\delta^{34}S$ of the sulfates of the TSR is similar, the $\delta^{34}S$ of the TSR solid bitumen can be used to show the extent of TSR

Data Availability

The sulfur isotope composition of solid bitumen and anhydrite data used to support the findings of this study are included within the article.

Conflicts of Interest

The authors declare that they have no conflicts of interest.

Acknowledgments

This study was supported by the National Natural Science Foundation of China (U1663210, 41672122), the Strategic Priority Research Program of the Chinese Academy of Sciences (XDA14010306), the National Science and Technology Major Project (2017ZX05005-003-003), and the China Scholarship Council. We acknowledge the support that was provided by Dr. Fenfang Wu from the California Institute of Technology for sulfur isotope analysis. We thank an anonymous reviewer's critical and constructive reviews to improve the quality of this article.

References

[1] H. G. Machel, H. R. Krouse, and R. Sassen, "Products and distinguishing criteria of bacterial and thermochemical sulfate reduction," *Applied Geochemistry*, vol. 10, no. 4, pp. 373–389, 1995.

[2] W. L. Orr, "Changes in sulfur content and isotopic ratios of sulfur during petroleum maturation–study of Big Horn Basin Paleozoic oils," *AAPG Bulletin*, vol. 58, pp. 2295–2318, 1974.

[3] O. Bildstein, R. H. Worden, and E. Brosse, "Assessment of anhydrite dissolution as the rate-limiting step during thermochemical sulfate reduction," *Chemical Geology*, vol. 176, no. 1-4, pp. 173–189, 2001.

[4] F. Hao, T. L. Guo, Y. M. Zhu, X. Y. Cai, H. Y. Zou, and P. P. Li, "Evidence for multiple stages of oil cracking and thermochemical sulfate reduction in the Puguang gas field, Sichuan Basin, China," *AAPG Bulletin*, vol. 92, no. 5, pp. 611–637, 2008.

[5] R. H. Worden, P. C. Smalley, and N. H. Oxtoby, "The effects of thermochemical sulfate reduction upon formation water salinity and oxygen isotopes in carbonate gas reservoirs," *Geochimica et Cosmochimica Acta*, vol. 60, no. 20, pp. 3925–3931, 1996.

[6] P. P. Li, F. Hao, X. S. Guo et al., "Origin and distribution of hydrogen sulfide in the Yuanba gas field, Sichuan Basin, Southwest China," *Marine and Petroleum Geology*, vol. 75, pp. 220–239, 2016.

[7] H. G. Machel, "Bacterial and thermochemical sulfate reduction in diagenetic settings–old and new insights," *Sedimentary Geology*, vol. 140, no. 1-2, pp. 143–175, 2001.

[8] S. Nöth, "High H_2S contents and other effects of thermochemical sulfate reduction in deeply buried carbonate reservoirs: a review," *Geologische Rundschau*, vol. 86, no. 2, pp. 275–287, 1997.

[9] H. E. King, C. C. Walters, W. C. Horn et al., "Sulfur isotope analysis of bitumen and pyrite associated with thermal sulfate reduction in reservoir carbonates at the Big Piney–La Barge production complex," *Geochimica et Cosmochimica Acta*, vol. 134, pp. 210–220, 2014.

[10] R. H. Worden, P. C. Smalley, and A. E. Fallick, "Sulfur cycle in buried evaporites," *Geology*, vol. 25, no. 7, pp. 643–646, 1997.

[11] R. H. Worden, P. C. Smalley, and S. A. Barclay, "H_2S and diagenetic pyrite in North Sea sandstones: due toTSR or organic sulphur compound cracking?," *Journal of Geochemical Exploration*, vol. 78-79, pp. 487–491, 2003.

[12] F. V. Acholla and W. L. Orr, "Pyrite removal from kerogen without altering organic matter: the chromous chloride method," *Energy and Fuels*, vol. 7, no. 3, pp. 406–410, 1993.

[13] C. F. Cai, K. K. Li, A. L. Ma et al., "Distinguishing Cambrian from Upper Ordovician source rocks: evidence from sulfur isotopes and biomarkers in the Tarim Basin," *Organic Geochemistry*, vol. 40, no. 7, pp. 755–768, 2009.

[14] C. F. Cai, K. K. Li, Y. M. Zhu et al., "TSR origin of sulfur in Permian and Triassic reservoir bitumen, East Sichuan Basin, China," *Organic Geochemistry*, vol. 41, no. 9, pp. 871–878, 2010.

[15] Y. Y. Kadıoğlu, S. Karaca, and S. Bayrakçeken, "Kinetics of pyrite oxidation in aqueous suspension by nitric acid," *Fuel Processing Technology*, vol. 41, no. 3, pp. 273–287, 1995.

[16] W. L. Orr, "Kerogen/asphaltene/sulfur relationships in sulfur-rich Monterey oils," *Organic Geochemistry*, vol. 10, no. 1-3, pp. 499–516, 1986.

[17] C. F. Cai, Z. Y. Xie, R. H. Worden, G. Y. Hu, L. S. Wang, and H. He, "Methane-dominated thermochemical sulphate reduction in the Triassic Feixianguan Formation East Sichuan Basin, China: towards prediction of fatal H_2S concentrations," *Marine and Petroleum Geology*, vol. 21, no. 10, pp. 1265–1279, 2004.

[18] J. Li, Z. Y. Xie, J. X. Dai, S. C. Zhang, G. Y. Zhu, and Z. L. Liu, "Geochemistry and origin of sour gas accumulations in the northeastern Sichuan Basin, SW China," *Organic Geochemistry*, vol. 36, no. 12, pp. 1703–1716, 2005.

[19] G. Y. Zhu, S. C. Zhang, Y. B. Liang, J. X. Dai, and J. Li, "Isotopic evidence of TSR origin for H_2S-rich gases in the Feixianguan Formation northeastern Sichuan Basin," *Science in China Series D*, vol. 48, no. 11, pp. 1960–1971, 2005.

[20] F. Hao, X. F. Zhang, C. W. Wang et al., "The fate of CO_2 derived from thermochemical sulfate reduction (TSR) and effect of TSR on carbonate porosity and permeability, Sichuan Basin, China," *Earth-Science Reviews*, vol. 141, pp. 154–177, 2015.

[21] P. P. Li, F. Hao, X. S. Guo, H. Y. Zou, X. Y. Yu, and G. W. Wang, "Processes involved in the origin and accumulation of hydrocarbon gases in the Yuanba gas field, Sichuan Basin, Southwest China," *Marine and Petroleum Geology*, vol. 59, pp. 150–165, 2015.

[22] G. M. Zhai, *Petroleum Geology of China (Vol. 10)*, Petroleum Industry Press, Beijing, 1989.

[23] Y. G. Wang, S. J. Chen, and S. Q. Xu, *The Formation Condition and the Prospecting Technology of the Gas Reservoir in Paleozoic and Upper Proterozoic in Sichuan Basin*, Petroleum Industry Press, Beijing, 2001.

[24] J. H. Du, C. C. Xu, Z. C. Wang et al., *Natural Gas Exploration of Permian-Triassic Reef & Oolite in Sichuan Basin*, Petroleum Industry Press, Beijing, 2010.

[25] Y. S. Ma, S. C. Zhang, T. L. Guo, G. Y. Zhu, X. Y. Cai, and M. W. Li, "Petroleum geology of the Puguang sour gas field in the Sichuan Basin, SW China," *Marine and Petroleum Geology*, vol. 25, no. 4-5, pp. 357–370, 2008.

[26] Y. G. Wang, L. R. Du, Y. C. Wen, J. Zhang, and H. Y. Liu, "Origin of H_2S in Triassic Feixianguan formation gas pools, Northeastern Sichuan Basin, China," *Geochimica*, vol. 31, pp. 517–524, 2002.

[27] Y. M. Zhu, J. B. Wang, F. Hao, H. Y. Zou, and X. Y. Cai, "Geochemical charateristics and origin of natural gases from Xuanhan area, eastern Sichuan," *Chinese Journal of Geology (Scientia Geologica Sinica)*, vol. 43, pp. 518–532, 2008, (in Chinese).

[28] C. F. Cai, R. H. Worden, S. H. Bottrell, L. S. Wang, and C. C. Yang, "Thermochemical sulphate reduction and the generation of hydrogen sulphide and thiols (mercaptans) in Triassic carbonate reservoirs from the Sichuan Basin, China," *Chemical Geology*, vol. 202, no. 1-2, pp. 39–57, 2003.

[29] A. Kampschulte and H. Strauss, "The sulfur isotopic evolution of Phanerozoic seawater based on the analysis of structurally substituted sulfate in carbonates," *Chemical Geology*, vol. 204, no. 3-4, pp. 255–286, 2004.

[30] C. F. Cai, L. Xiang, Y. Y. Yuan et al., "Sulfur and carbon isotopic compositions of the Permian to Triassic TSR and non-TSR altered solid bitumen and its parent source rock in NE Sichuan Basin," *Organic Geochemistry*, vol. 105, pp. 1–12, 2017.

[31] S. R. Kelemen, C. C. Walters, P. J. Kwiatek et al., "Distinguishing solid bitumens formed by thermochemical sulfate reduction and thermal chemical alteration," *Organic Geochemistry*, vol. 39, no. 8, pp. 1137–1143, 2008.

[32] B. K. Manzano, M. G. Fowler, and H. G. Machel, "The influence of thermochemical sulphate reduction on hydrocarbon composition in Nisku reservoirs, Brazeau river area, Alberta, Canada," *Organic Geochemistry*, vol. 27, no. 7-8, pp. 507–521, 1997.

[33] W. L. Orr, "Geologic and geochemical controls on the distribution of hydrogen sulfide in natural gas," in *Advances in Organic Geochemistry 1975*, R. Campos and J. Goni, Eds., pp. 571–597, Enadisma, Madrid, 1977.

[34] T. W. Zhang, G. S. Ellis, C. C. Walters, S. R. Kelemen, K. S. Wang, and Y. C. Tang, "Geochemical signatures of thermochemical sulfate reduction in controlled hydrous pyrolysis experiments," *Organic Geochemistry*, vol. 39, no. 3, pp. 308–328, 2008.

[35] G. D. Jones and Y. Xiao, "Dolomitization, anhydrite cementation, and porosity evolution in a reflux system: insights from reactive transport models," *AAPG Bulletin*, vol. 89, no. 5, pp. 577–601, 2005.

[36] H. Rahimpour-Bonab, B. Esrafili-Dizaji, and V. Tavakoli, "Dolomitization and anhydrite precipitation in Permo-Triassic carbonates at the South Pars gasfield, offshore Iran: controls on reservoir quality," *Journal of Petreleum Geology*, vol. 33, no. 1, pp. 43–66, 2010.

[37] L. Jiang, C. F. Cai, R. H. Worden, K. K. Li, and L. Xiang, "Reflux dolomitization of the Upper Permian Changxing Formation and the Lower Triassic Feixianguan Formation, NE Sichuan Basin, China," *Geofluids*, vol. 13, no. 2, 245 pages, 2013.

[38] K. K. Li, C. F. Cai, D. J. Hou et al., "Origin of high H_2S concentrations in the Upper Permian Changxing reservoirs of the Northeast Sichuan Basin, China," *Marine and Petroleum Geology*, vol. 57, pp. 233–243, 2014.

[39] X. F. Zhang, *The Reservoir Formation and Preservation of Lower Triassic Feixianguan Formation, Northeastern Sichuan Basin, [Ph.D Thesis]*, Chinauniversity of Petroleum, Beijing, 2009.

[40] P. E. Videtich, "Dolomitization and H_2S generation in the Permian Khuff Formation, offshore Dubai, U.A.E," *Carbonates and Evaporites*, vol. 9, no. 1, pp. 42–57, 1994.

[41] R. H. Worden, P. C. Smalley, and N. H. Oxtoby, "Gas souring by thermochemical sulfate reduction at 140°C," *AAPG Bulletin*, vol. 79, pp. 854–863, 1995.